

Dynamic Interactions of Fluorescently Labeled Microtubule-associated Proteins in Living Cells

TALMA SCHERSON,* THOMAS E. KREIS,[‡] JOSEPH SCHLESSINGER,[‡]
URIEL Z. LITTAUER,* GARY G. BORISY,[§] and BENJAMIN GEIGER[‡]

Departments of *Neurobiology and [‡]Chemical Immunology, The Weizmann Institute of Science, Rehovot 76100, Israel; and [§]Laboratory of Molecular Biology, University of Wisconsin, Madison, Wisconsin 53706. Dr. Kreis' present address is European Molecular Biology Laboratories, Heidelberg, Federal Republic of Germany.

ABSTRACT Microtubule-associated proteins (MAPs) from calf brain were fluorescently labeled with 6-iodoacetamido fluorescein (I-AF). The modified MAPs (especially enriched for MAP₂) were fully active in promoting tubulin polymerization in vitro and readily associated with cytoplasmic filaments when microinjected into living cultured cells. Double-labeling experiments indicated that the microinjected AF-MAPs were incorporated predominantly, if not exclusively, into cytoplasmic microtubules in untreated cells or paracrystals induced within vinblastine-treated cells. Similar results were obtained with different cell types (neuronal, epithelial, and fibroblastic) of diverse origin (man, mouse, chicken, and rat kangaroo). Mobility measurements of the microinjected AF-MAPs using the method of fluorescence-photobleaching recovery (FPR) revealed two populations of AF-MAPs with distinct dynamic properties: One fraction represents the soluble pool of MAPs and is mobile with a diffusion coefficient of $D = 3 \times 10^{-9}$ cm²/s. The other fraction of MAPs is associated with the microtubules and is essentially immobile on the time scale of FPR experiments. However, it showed slow fluorescence recovery with an apparent half time of ~5 min.

The slow recovery of fluorescence on defined photobleached microtubules occurred most probably by the incorporation of AF-MAPs from the soluble cytoplasmic pool into the bleached area. The bleached spot on defined microtubules remained essentially immobile during the slow recovery phase. These results suggest that MAPs can associate in vivo with microtubules of diverse cell types and that treadmilling of MAP₂-containing microtubules in vivo, if it exists, is slower than 4 μ m/h.

Microtubules are a widely distributed class of cytoskeletal filaments, believed to be involved in a variety of dynamic cellular processes. Among these are cell division, secretion, intracellular transport, maintenance of cell shape, etc. (for review, see reference 1). Biochemical and immunocytochemical studies have shown that microtubules are predominantly composed of α - and β -tubulin heterodimers as well as of microtubule-associated proteins (MAPs)¹ (2-9). There are two major heat stable groups of MAPs that co-purify with brain microtubules during in vitro assembly-disassembly cycles: the

higher molecular weight MAP₂ (molecular weight 270,000) and the tau factors, a group of four to six polypeptides with molecular weights between 55,000 and 62,000 (5, 10). In vitro, both classes of MAPs facilitate overall tubulin assembly by promoting initiation of polymerization as well as increasing the rate of microtubule elongation (2-3, 10-11).

Since individual microtubules are not contractile in nature, it is conceivable that generation of movement by microtubules is based either on polymerization-depolymerization events (12), on sliding movements between individual microtubules (13-14) or on interactions with other cell organelles (15). Polymerization-dependent movements could be involved in the generation of force by at least two mechanisms: (a) elongation of shortening at one or both ends of the microtubule (16) and (b) treadmilling, namely the net addition of tubulin heterodimers at one end of the microtubules (plus

¹ Abbreviations used in this paper: AF, acetamido fluorescein; FPR, fluorescence-photobleaching recovery; MAP, microtubule-associated proteins; NBr10-A, mouse neuroblastoma \times buffalo rat liver hybrid cells; PC, phosphocellulose; RB200SC, lissamine rhodamine B sulfonfyl chloride.

end) and a similar net dissociation at the minus end (17–20). The treadmill model implies that at steady state there is a flux of tubulin subunits along the filaments from the plus end to the minus end. The treadmill model was based predominantly on *in vitro* reconstitution studies (16–18, 21) as well as on theoretical considerations (22).

There is now increasing evidence suggesting that microtubules interact with other cytoskeletal structures such as intermediate filaments, or with cellular organelles including mitochondria or pigment granules (23–25). Although the molecular nature of these interactions is not clear, it has been suggested that at least some of them might be mediated by MAP molecules (26–27). Moreover, it has been speculated that organelle translocation along microtubules could be related to a treadmill process (19).

In an attempt to study treadmill and the dynamic properties of microtubules in living cells, we prepared fluorescently labeled derivatives of MAPs (mostly MAP₂) and microinjected them into living cells. It was our hope that labeled MAPs might be used as dynamic markers for native microtubules. Microinjection of fluorescently tagged molecules has been successfully used previously to visualize *in vivo* different cytoskeletal elements, including actin, α -actinin, vinculin, and tubulin (28–32). Moreover, microinjection of fluorescently labeled proteins has been combined recently with fluorescence-photobleaching recovery (FPR), to determine the intracellular mobility of actin, α -actinin, and vinculin in cultured cells (33, 34). Using a similar approach we show here that MAP₂ maintains a dynamic equilibrium between “cytoskeletal” and “soluble” pools. In living cells, fluorescently labeled MAPs appear to be associated primarily (if not exclusively) with microtubules. Moreover, bleached spots along fluorescently labeled microtubules do not show “movement” along the filaments. This suggests that treadmill, at least as a process that is supposed to mobilize the entire microtubule structure and possibly different cellular organelles associated with it, either does not occur in the living cultured cells tested or else is limited to a maximal rate of $\sim 4 \mu\text{m/h}$. Preliminary results of some of these studies were previously presented (35).

MATERIALS AND METHODS

Cells and Tissue Culture: Embryonic chicken gizzard cells were prepared and cultured in Dulbecco's modified Eagle's medium containing 10% fetal calf serum. Mouse neuroblastoma \times buffalo rat liver (NBr10-A) hybrid cells (36) were kindly provided by Dr. M. Nirenberg. For microinjection NBr10-A cells were plated on glass coverslips (coated overnight with 10 $\mu\text{g/ml}$ of polylysine solution) in Dulbecco's modified Eagle's medium containing 2% fetal calf serum, 100 μM hypoxanthine 1 μM aminopterin, 16 μM thymidine, and 1 mM N⁶, O²-dibutyryl adenosine 3':5'-cyclic monophosphate for at least 3 d to induce neurite extension. Confluent rat kangaroo PtK₂ cells were plated onto glass coverslips and used within 1 or 2 d of their incubation. 6-Iodoacetamidofluorescein (I-AF) was obtained from Molecular Probes (Plano, TX) and GTP from Sigma Chemical Co. (St. Louis, MO).

Microinjection Procedures: Microinjection of fluorescently-labeled proteins into cells plated onto glass coverslips was performed as previously described (37), using thin wall capillaries (type GC 150 TF-15, Clark Electromedical Instruments, Pangbourne, UK).

Preparation of AF-MAPs: Calf brain microtubules were prepared by two cycles of assembly and disassembly (38). The microtubule pellets obtained were resuspended in buffer (0.3 M 4-morpholino-ethane sulfonic acid, pH 6.6, 1 mM EGTA, 0.1 mM EDTA, 1 mM MgCl₂) without dithiothreitol (Cleland's reagent). The protein concentration was adjusted to 20 mg/ml and the microtubules modified at 4°C by addition of 3 mol of I-AF per 10⁵ g of total microtubular protein (diluted from a freshly-prepared 10 mM stock solution in dimethyl sulfoxide). After 10 min at room temperature the reaction was quenched with 2 mM dithiothreitol. NaCl was then adjusted to 0.8 M and the microtubules incubated at 4°C for 1 h. Tubulin, MAP₁, and some minor protein

components in the microtubule-protein mixture were denatured by heating for 5 min in a boiling water bath and were removed by centrifugation at 6,000 g in a Sorvall centrifuge (Brinkmann Instruments, Inc., Westbury, NJ). The proteins present in the supernatant were concentrated by ammonium sulfate precipitation (40% saturation) and desalted over a Sephadex G-50 fine column in 0.3 M KCl in the 4-morpholino-ethane sulfonic acid buffer. Aliquots were immediately frozen at -70°C .

Fluorescence Microscopy and FPR: Fluorescence microscopy was performed with a Zeiss photomicroscope III or Universal Zeiss Microscope equipped with filter sets for selective observation of either fluorescein or rhodamine fluorescence. Image-intensified microscopy was carried out with a Universal Zeiss Microscope (Neofluar 63, 1.25 oil immersion objective) equipped with either a silicon-intensified target camera (RCA, TC 1030/4) or with an intensified silicon-intensified target camera connected to a time lapse video recorder (Panasonic VTR-NV-8030) and a 9-in TV monitor. Mobility measurements were performed using the fluorescence photobleaching recovery apparatus that was previously described (33). A focused laser beam (argon, 514 nm) was used to photobleach and monitor the fluorescence of a small area of the cell according to published procedures (33). The diffusion coefficients were derived from the FPR curves according to Axelrod et al. (39). Incomplete fluorescence recovery was interpreted as an indication that a fraction of the fluorophore is “immobile” on the time scale of FPR experiments ($D < 3 \times 10^{-12} \text{ cm}^2/\text{s}$). Intensified cellular images were photographed directly from the monitor with a Polaroid camera on type 665 polaroid films.

Other Methods: Protein concentrations were estimated spectrophotometrically from the absorbance at 280 and 260 nm. The fluorescein concentration was estimated from the absorbance at 495 nm (28). SDS PAGE was performed according to the method of Laemmli (41) using 8% polyacrylamide.

RESULTS

Fluorescent Labeling of MAPs

Various approaches were attempted for the conjugation of fluorophores to the different protein constituents of microtubules. These included the separation of MAPs from tubulin by phosphocellulose (PC) chromatography and the subsequent labeling with different fluorophores including dichlorotriazinyl amino fluorescein, lissamine-rhodamine sulfonyl chloride (RB200SC), and I-AF. Alternatively, microtubules were reconstituted by mixing tubulin and MAPs, then labeled, disassembled, and fractionated by PC chromatography. However, the procedure which was finally selected for the present studies involved the conjugation of I-AF to microtubules as specified in Materials and Methods.

A gel electrophoretic pattern of the fluorescently labeled MAPs is shown in Fig. 1. Densitometric scanning of polyacrylamide slab gels indicated that the major fluorescently labeled band corresponding to about 70% of the fluorescence (also the major band by Coomassie Brilliant Blue staining) was MAP₂ (arrowhead). A low level of labeling coincided with the tau factors (brackets). It should be emphasized that tubulin was completely removed by this treatment. This procedure gave superior fluorescent labeling of MAPs as compared to other methods mentioned above. We have found that conjugation with either dichlorotriazinyl amino fluorescein or RB200SC hampered the capacity of the labeled MAPs to coassemble with brain microtubules. Moreover, separation of labeled MAPs from tubulin by PC chromatography was incomplete and relatively inefficient.

Interaction of AF-MAPs with Tubulin

The fluorescently labeled MAPs were examined for their capacity to promote polymerization of PC tubulin *in vitro*. The results, as shown in Fig. 2 indicated that AF-MAPs were as active as the native protein in stimulating tubulin polymerization. These experiments strongly suggested that the conjugation of AF to MAPs (especially MAP₂) did not alter their mode of interaction with microtubules. To rule out the pos-

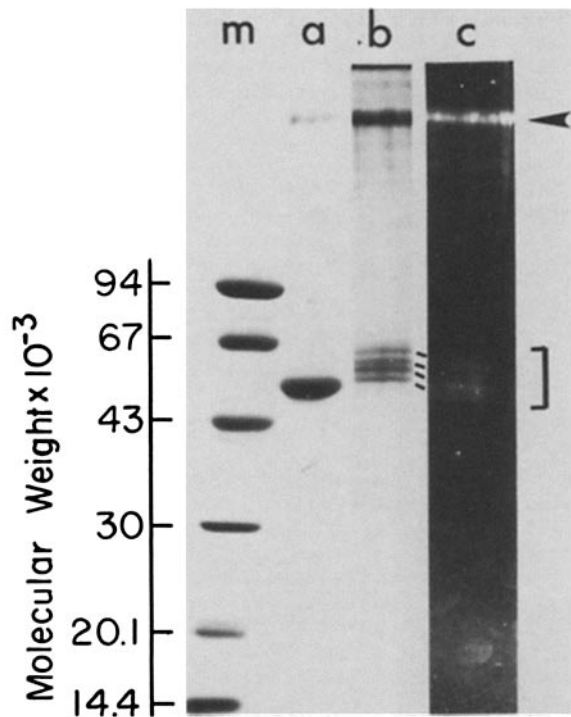


FIGURE 1 SDS-PAGE of AF-MAPs. Calf brain microtubules purified by two cycles of assembly-disassembly and labeled with 6-iodoacetamido fluorescein as described. The labeled microtubules were dissolved at 4°C and then tubulin, MAP₁, and some minor proteins were removed by heating and centrifugation. Aliquots of AF-MAPs were immediately frozen at -70°C. (m-b) Coomassie-Brilliant-Blue-stained gels; molecular weight markers (phosphorylase b: 94, bovine serum albumin; 67, ovalbumin; 43, carbonic anhydrase; 31, (Pharmacia, Sweden); (a) Calf brain microtubules (b) purified MAPs. (c) Fluorescence pattern of the conjugated AF-MAPs (the same as b) but visualized by ultraviolet illumination.

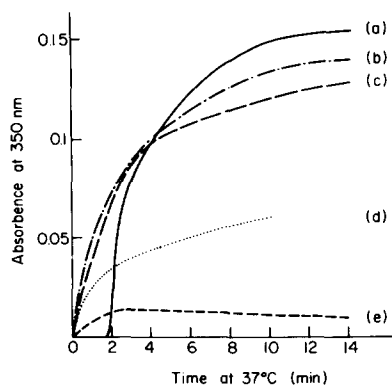


FIGURE 2 Kinetics of reconstituted microtubule polymerization determined by turbidimetric assay. PC-Tubulin and either AF-labeled or native MAPs mixtures were prepared at 4°C, GTP and dithiothreitol were added to a final concentration of 1 mM and the mixtures were immediately loaded into a quartz curvette in a Gilford Spectrophotometer prewarmed to 37°C. Changes in turbidity were followed at 350 nm. The kinetic curves correspond to (a) calf brain total microtubule proteins (2 mg/ml), (b) PC-tubulin (2 mg/ml) mixed with purified native MAPs (0.16 mg/ml); (c) PC-tubulin (2 mg/ml) mixed with AF-MAPs (0.16 mg/ml), (d) PC-tubulin (1 mg/ml) mixed with AF-MAPs (0.16 mg/ml) and (e) PC-tubulin (2 mg/ml) alone.

sibility that an unlabeled fraction in the AF-MAPs preparation was potentiating polymerization of PC-purified tubulin while the labeled protein was inactive, we directly examined the *in vitro* assembled microtubules under the fluorescence microscope. The results presented in Fig. 3A indicate that the fluorescence was associated with bundles of filaments of variable lengths. These *in vitro* reassembled AF-microtubules underwent rapid depolymerization when incubated at 2–4°C for several minutes (Fig. 3B). We conclude, therefore, that AF-MAPs resemble closely native MAPs with respect to their interaction with microtubules.

Spatial Distribution of Microinjected AF-MAPs in Living Cultured Cells

AF-MAPs were microinjected into several types of cultured cells, including chicken gizzard fibroblasts, PtK₂, and neuroblastoma-liver hybrid NBr10-A cells. Within 30 min after microinjection the injected AF-MAPs became associated with filamentous structures throughout the cells. Typical examples for the incorporation of AF-MAPs into the microtubular system are shown in Fig. 4. In the case of NBr10-A cells (Fig. 4A) the fluorescence within the cell body was often intense and individual filaments could hardly be resolved. Nevertheless, filamentous structures were detected in many of the cellular processes (see arrows in Fig. 4A). The PtK₂ (Fig. 4B) and chicken gizzard cells (Fig. 4C) were more spread and individual filaments could be resolved in the cytoplasm. Often

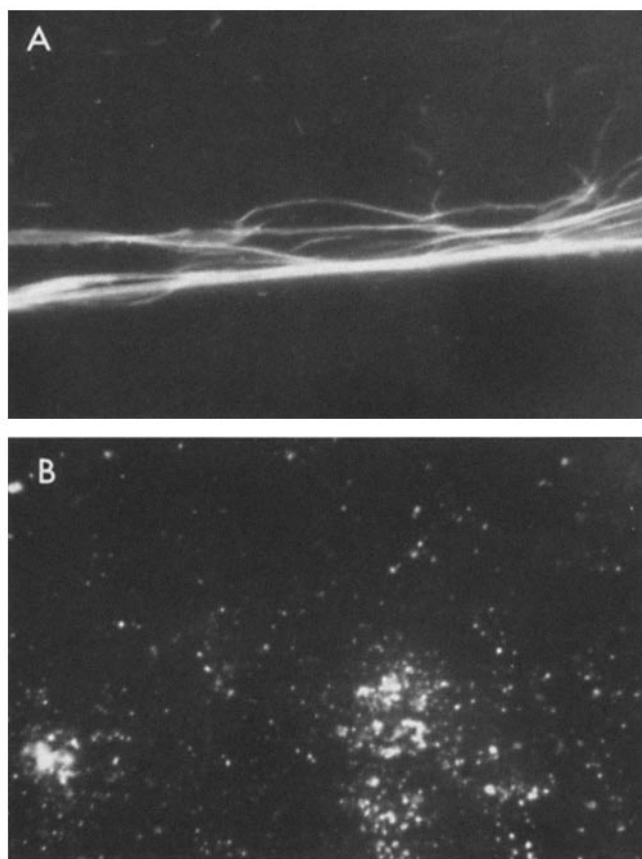


FIGURE 3 Visualization of fluorescent microtubules derived *in vitro* from mixing PC-tubulin (2 mg/ml) and AF-MAPs (0.16 mg/ml) by fluorescence microscopy (A). Cold treatment of the same preparation (B) for 10 minutes, most fibrillary structures disappeared. $\times 315$.

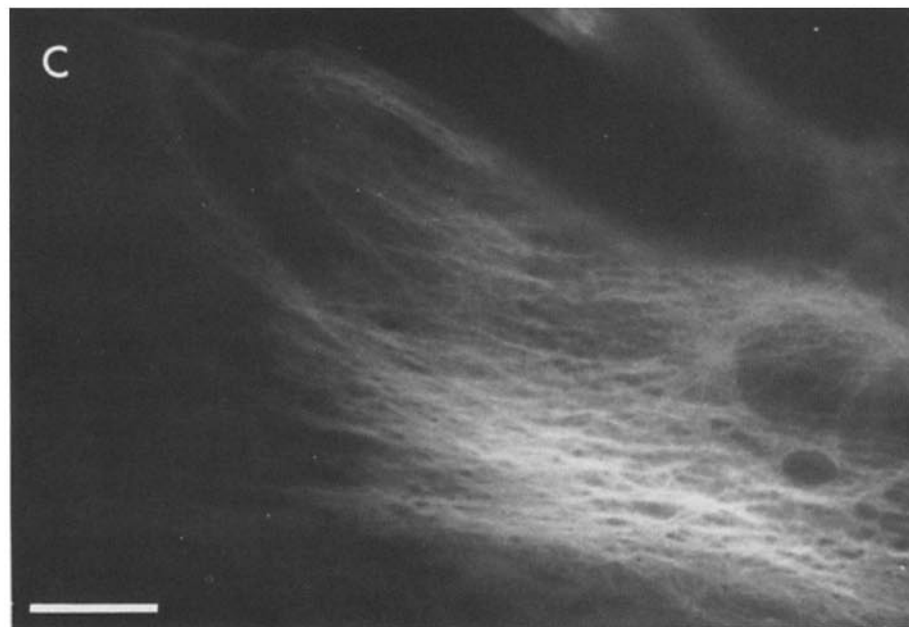
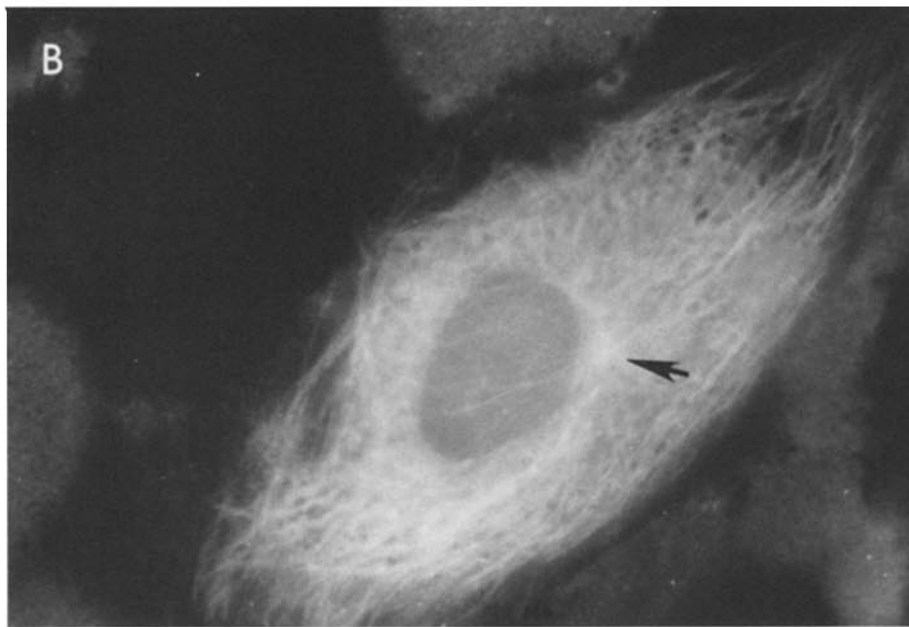
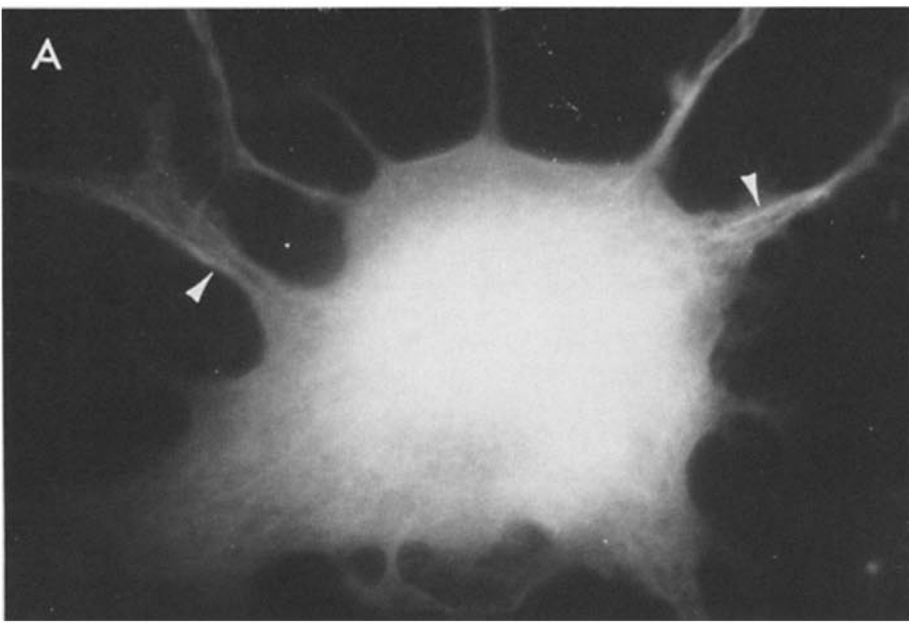


FIGURE 4 Distribution of AF-MAPs microinjected into living cells. (A) NBr10-A cell, 3 h after microinjection. The association of AF-MAPs with filaments is clearly resolved in flat areas such as the neurite extensions (arrows). (B) A PtK₂ cell 3 h after microinjection. AF-MAPs associate with cytoplasmic filaments as well as with a structure resembling microtubule organizing center (indicated by the arrow). (C) 1A chicken gizzard cell visualized ~3 h after injection. AF-MAP₂ becomes associated with well-defined filaments. Bar, 10 μ m.

a structure similar to a microtubule-organizing center could be detected near the nucleus (arrowhead in Fig. 4B).

Double-labeling experiments were also performed to examine whether AF-MAPs were indeed bound to distinct microtubule structures. According to our experience, MAP₂ readily dissociates from microtubules upon extraction with detergents and fixation with formaldehyde (42, 43). Therefore, we have employed here the following procedure to compare the location of the injected AF-MAPs with that of microtubules. The fluorescence of the former was photographed when the cells were still alive, then the cells were fixed and the microtubules were visualized by indirect immunofluorescence with antibodies directed against tubulin and rhodamine goat anti-rabbit antibodies. The overall pattern of the fluorescence in the two sets of pictures appeared similar. However, in most cases the microtubular networks were too dense to allow for a precise comparison of individual fibers. We have therefore treated the cells with colchicine (10 μg/ml) for 30 min. In PtK₂, this treatment brought about a reduction in the number of AF-MAP-labeled filaments and the remaining ones could be easily discerned as shown in Fig. 5. These cells were photographed, then fixed, permeabilized, and fluorescently immunolabeled for tubulin. Comparison of these patterns indicated that they were essentially identical. The small differences are attributed to minor spatial changes that might have occurred during fixation. It should be emphasized that under these conditions vimentin filaments formed "juxtannuclear caps" (not shown) that had no spatial relationships to the microinjected AF-MAPs. Furthermore, treatment of PtK₂ cells with vinblastine resulted in a drastic reorganization of the microtubular and intermediate filament systems; the former lost their filamentous structure and formed cytoplasmic paracrystals, while the latter (especially vimentin filaments) were aggregated into thick bundles. This could be visualized by indirect immunofluorescent labeling for vimentin (Fig. 6A and tubulin (Fig. 6B). The same experiments, when performed with cells, microinjected with AF-MAPs, resulted in a clear cut association of microinjected proteins with the vinblastine-induced paracrystals (Fig. 6C).

FPR Experiments with Cultured Cells Microinjected with AF-MAPs

The observation that soluble fluorescently labeled MAPs become readily associated with the cytoplasmic microtubular network strongly suggested that there were free sites for MAP binding on intact microtubules and that the putative endogenous MAPs in the injected cells could be readily exchanged with the fluorescently labeled MAPs. This consideration applies both to cells that contain endogenous MAP₂(NBr10-A) and to cells in which endogenous MAP₂ could not be detected (PtK₂, chicken gizzard) (see Discussion). To gain further information concerning the dynamic properties of MAPs in the soluble pool as well as those molecules that were bound to microtubules we have applied the laser photobleaching system. FPR experiments were performed on two different cell types, chicken gizzard cells and neuroblastoma hybrid NBr10-A cells displaying marked differences in morphology and microtubule organization. In chicken gizzard fibroblasts, dense networks of microtubules can be seen with arrays of filaments oriented in different directions. The NBr10-A cells on the other hand, and especially their neurite extensions contained bundles of microtubules in a parallel alignment. In

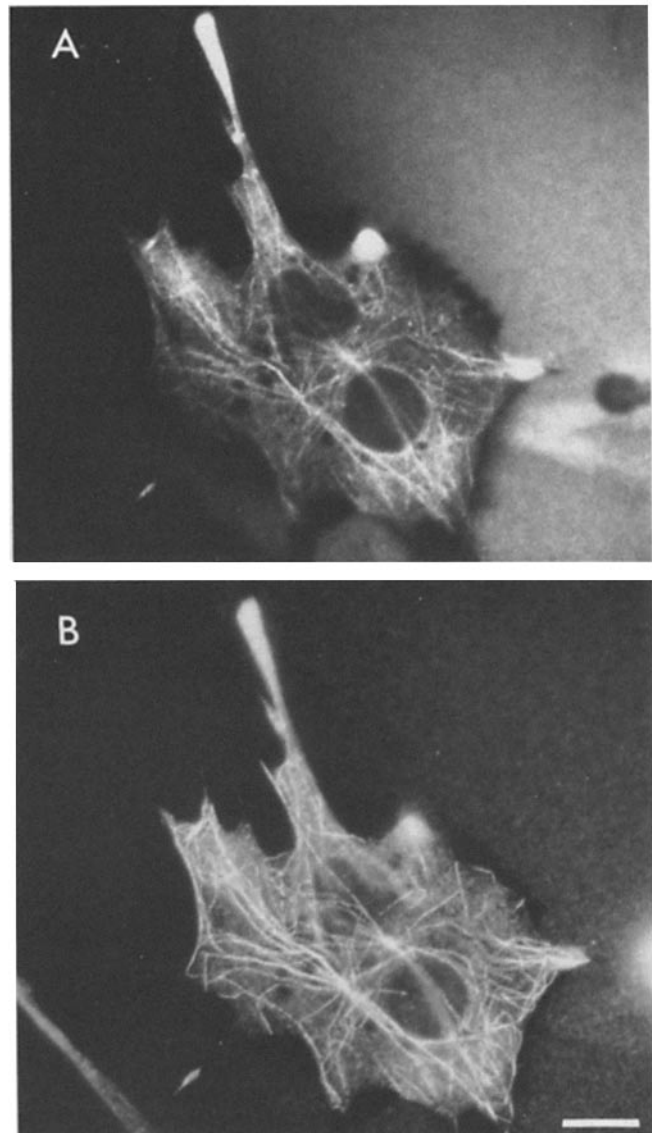


FIGURE 5 Comparison of the cellular distribution of microinjected AF-MAPs with colchicine-resistant microtubules. (A) Chicken gizzard cells microinjected with AF-MAP₂ and 3 h later treated with 10 μg/ml of colchicine for 30 min at 37°C. (B) The same cell permeabilized, fixed, and immunolabeled with tubulin antibodies. Notice that the pattern obtained with AF-MAP₂ and antitubulin labeling are essentially identical. Bar, 10 μm.

these cells we define domains that differ in the relative contents of cytoplasmic and of assembled microtubules. In the flat areas of chicken gizzard cells, we may distinguish between areas of sparse distribution of microtubules (*i* in Table I) and regions where dense arrays of fibers are seen (*ii*). With NBr10-A cells we distinguish in Table I between the thick perinuclear area (*iii*) and flat processes in which arrays of defined microtubules are observed (*iv*). As summarized in Table I, a control protein (fluorescein-labeled IgG) exhibited a virtually complete recovery of fluorescence in all the subcellular domains with diffusion coefficient (D) = $4.1\text{--}4.6 \times 10^{-9}$ cm²/s, (see also [33]). Analysis of FPR curves of the labeled MAPs revealed the existence of at least two populations of molecules with distinct mobilities: a mobile fraction in the cytoplasm with a similar diffusion coefficient to that of control protein (D = 3×10^{-9} cm²/s) and a fraction that was associated with

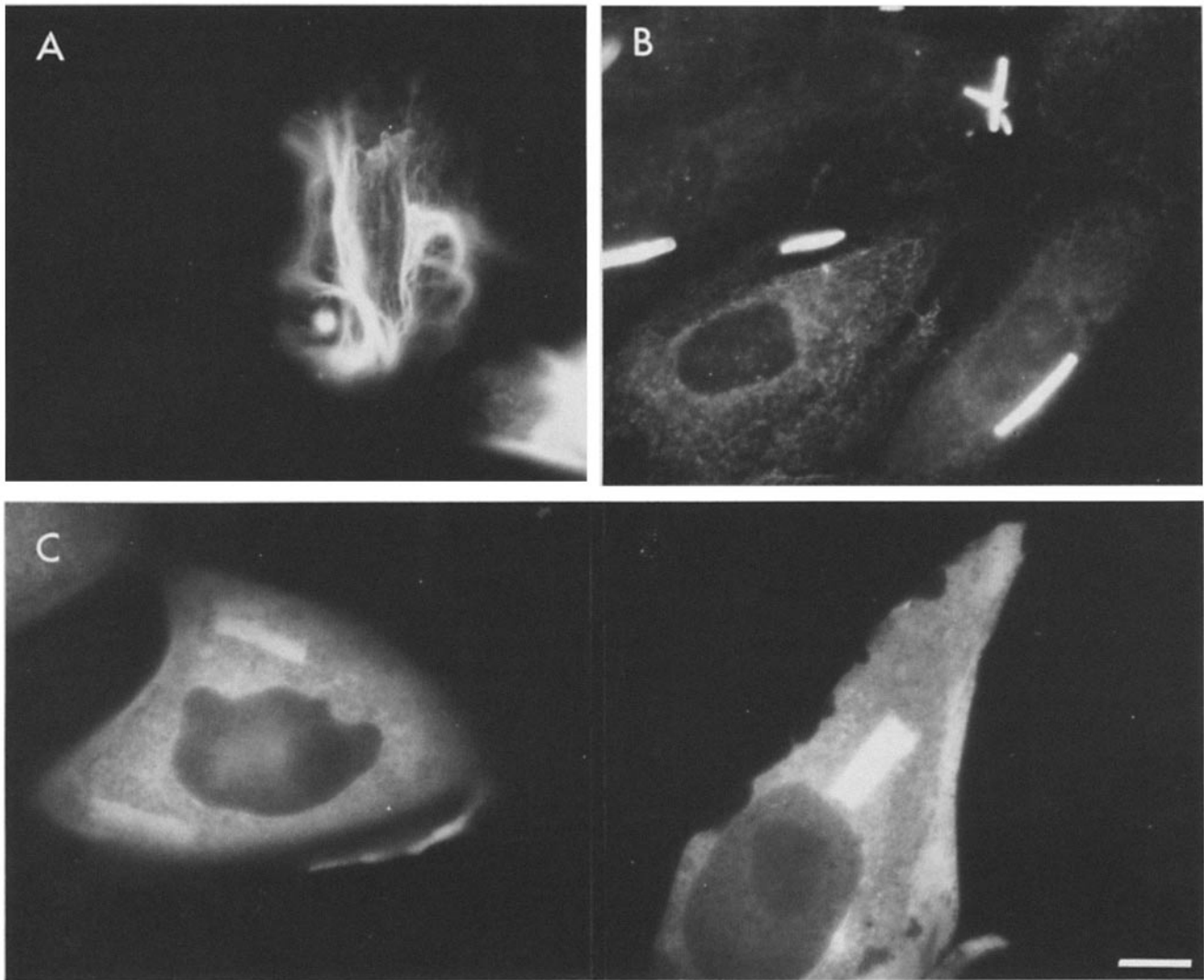


FIGURE 6 Association of AF-MAP₂ with vinblastine-induced paracrystals. PtK₂ cells were treated with 10 μ g/ml of vinblastine for 3 h at 37°C. The vimentin perinuclear bundles and tubulin-containing paracrystals were visualized in control cells by immunofluorescent labeling with antibodies to (A) antivimentin and (B) antitubulin. (C) The same experiments performed with cells microinjected with AF-MAP₂. Note the association of AF-MAP with vinblastine-induced paracrystals. Bar, 10 μ m.

labeled microtubules (20–50%) and that appeared to be immobile on the time scale of FPR experiments. Thus we conclude that the mobile fraction represents the soluble cytoplasmic pool surrounding the assembled microtubules.

Analysis of the Slow FPR of AF-MAPs Containing Microtubules

We have noticed that, in areas where a large fraction of AF-MAPs appeared as “immobile” on the time scale of FPR experiments, a slow recovery of fluorescence occurred within several minutes after photobleaching. In contrast to the fast component, the slow fluorescence recovery was independent of the size of the photobleached area (providing that it was small relative to the cell size) (33). To further explore the nature of this slow recovery, we performed additional experiments in the neurite extension of microinjected NBr10-A cells. We bleached a line across the microtubules within these neurites using a partially-attenuated laser beam. Subsequently, the fluorescence recovery into the bleached area was either quantitatively monitored with an attenuated laser beam

of the FPR system or qualitatively visualized by time-lapse cinematography with a sensitive image-intensification microscopy system (for details see reference 33). The recovery of fluorescence in the bleached area is demonstrated in Fig. 7. It shows an NBr10-A cell bleached on one of its processes, and subsequently visualized with the image-intensification system on the TV monitor at different time intervals after bleaching. Quantitative analysis indicated that the half time of fluorescence recovery ($\tau/2$) was reproducibly 5–7 min. The fluorescence recovery reached maximal values of ~80–90% of the initial fluorescence and therefore could still be resolved for 5–10 min after photobleaching. These observations further demonstrated that MAP₂ can be incorporated into preexisting microtubules.

No Evidence for Movement of Photobleached Spots on Defined Microtubules

Despite the relatively fast rate of fluorescence recovery ($\tau/2 \approx 5$ min) the photobleached segments on microtubule arrays could still be identified for an average of 7.5 min and in most

cases up to ~10 min after photobleaching. This property enabled us to examine whether the photobleached area apparently changed its position along the microtubules or remained immobile during this time period. These analyses were performed by measuring the position of the bleached spot relative to fixed reference points over the cell or the substrate, at various time intervals. The results of such experiments including those shown in Fig. 7 indicated that the recovery of fluorescence occurred at the site of bleaching and there was no evidence for movement of the bleached zone. We estimate that the minimum movement of the bleached

zone that we could detect was 0.5 μm , which was the diameter of the bleaching beam. Failure to detect any movement permits us to estimate an upper bound for the rate of treadmilling of 0.5 $\mu\text{m}/7.5 \text{ min} = 4 \mu\text{m}/\text{h}$.

DISCUSSION

In the present study we investigated the dynamic properties of microtubules in living cells by combination of microinjection and FPR measurements. We have attempted to answer the following questions: (a) What are the native associations of MAPs in living cells (are they associated only with microtubules or also with other cellular organelles)? (b) Can brain MAPs interact with the microtubular system from diverse cell types or is their binding restricted to neuronal cells only? (c) What are the dynamic interrelationships of MAPs and microtubules in living cells? (d) Is there a flux of microtubular components, such as MAPs along microtubules under steady-state conditions, as a consequence of a treadmilling process?

The experimental approaches presented here are useful not only for measurements of the cellular dynamics of MAPs, but also carry significant advantages for the determination of their spatial distribution in vivo. Many recent studies on the organization of the cytoplasm in eucaryotic cells have suggested that different cytoskeletal networks may be closely interrelated, forming an integrated filamentous framework. MAP₂ is known to be laterally associated with the periphery of microtubules with its side arm extended away from the microtubular backbone. It has thus been suggested that MAP₂ might mediate the linkage between microtubules and other filamentous networks or cellular organelles (23–25). Another advan-

TABLE 1
FPR Measurements with Microinjected AF-MAPs in Living Cultured Cells

Protein	Cell type	$D \times 10^{-9}$ (cm^2/s)	Mobile fraction %
F1-IgG	Chicken gizzard	4.1 ± 0.8	>90
F1-IgG	NBr10-A	4.6 ± 1.0	>90
F1-IgG	NBr10-A	4.3 ± 0.8	>90
AF-MAPs	Chicken gizzard (i)	2.8 ± 0.4	>75%
AF-MAPs	Chicken gizzard (ii)	3.1 ± 0.4	50–70%
AF-MAPs	NBr10-A (iii)	2.9 ± 0.3	>85%
AF-MAPs	NBr10-A (iv)	2.9 ± 0.6	65–80%

Fluorescein-conjugated goat immunoglobulin (1 mg/ml) and AF-labeled MAPs (1–5 mg/ml) were injected and the apparent diffusion coefficient as well as the fractional mobilities calculated. Measurements were performed in distinct cellular domains: (i) areas with sparsely distributed microtubules; (ii) flat areas with dense arrays of microtubules; (iii) perinuclear areas; (iv) elongated cellular processes.

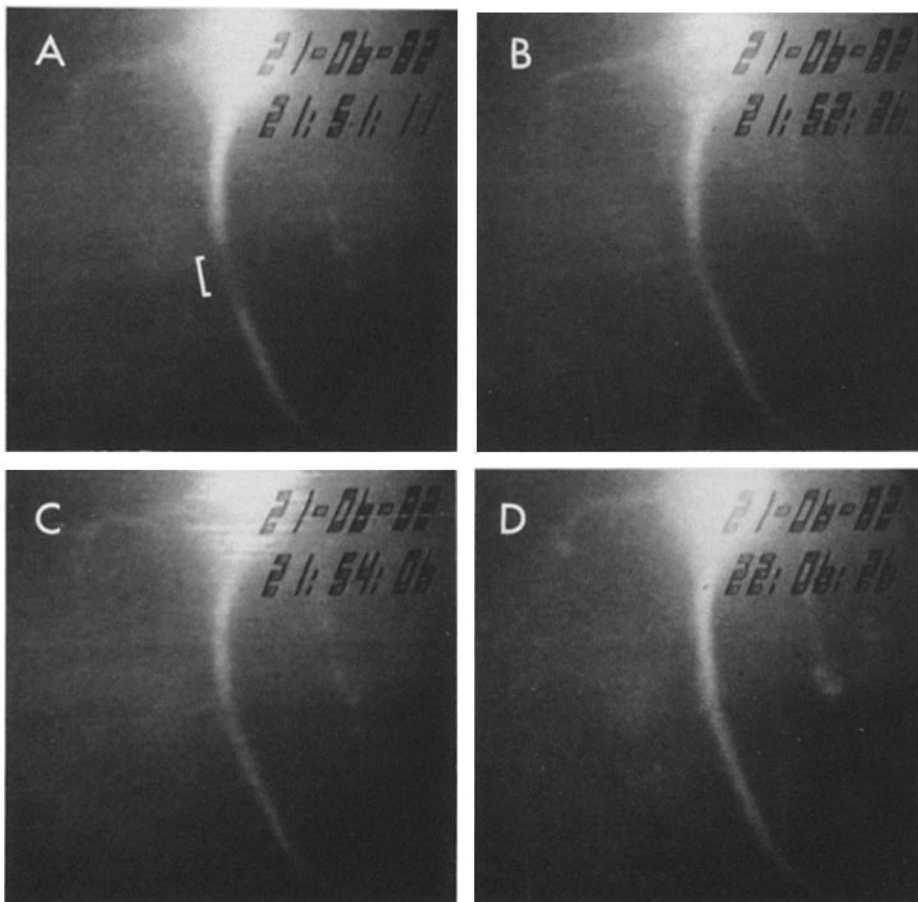


FIGURE 7 Slow fluorescence recovery after photobleaching of AF-MAP₂-labeled microtubules in a neurite extension of NBr10-A cell. A line was bleached across the microtubules by the laser beam (1.5- μm diameter). The fluorescent image of the cell was continuously monitored by the silicon-intensified target camera and recorded by time-lapse video cinematography. Polaroid pictures were taken from the TV-monitor at different intervals after bleaching: (A) Time zero. (B) 1.25 min after bleaching. (C) 3 min. (D) 15 min. The bleached area, indicated by the bracket recovered with a $\tau/2$ of ~5 min. $\times 650$.

tage of the microinjection approach is related to the apparent alterations in the native distribution of MAP₂ upon fixation and permeabilization, a step which is essential for immunofluorescent labeling (44). This preparation artifact could be circumvented by microinjection and visualization of the intracellular structures in the living cells.

Obviously the experimental approach described here may be useful only if the labeled microinjected proteins faithfully represent the behavior of their native unmodified counterparts. Three main aspects should be considered while interpreting the results obtained with the microinjected AF-MAPs: (a) Which of the polypeptides in the AF-MAPs preparation are biologically active? (b) Does the modification alter significantly the binding properties of MAPs to tubulin or to other cytoplasmic elements? (c) Are the normal stoichiometric relationships between MAPs and tubulin artificially altered in cells microinjected with MAPs?

We prepared fluorescently labeled derivatives of MAPs by several alternative procedures. It is obviously desirable to label only one single protein (MAP₂ or individual tau polypeptides). However, such preparations were poorly active as determined by our *in vitro* and *in vivo* criteria. In the preparations we used for microinjection ~70% of the fluorescence was associated with MAP₂. Moreover, when separated by gel filtration the MAP₂ fraction was functionally active (though relatively unstable) while no activity was associated with isolated labeled tau polypeptides. These observations suggest that the experiments described here reflect predominantly the behavior of MAP₂.

A related question is concerned with the effect of modification on the putative interactions of the microinjected AF-MAPs with tubulin. Our experience with different labeling procedures indicated that amino group reactive fluorophores (trichlorotriazinyl amino fluorescein and RB200SC) were inferior to the sulfhydryl-reactive iodoacetamido derivative used here. We also noticed that modification with I-AF of assembled microtubules resulted in labeled MAPs that were more active than those similarly labeled at the disassembled state.

As for the quantitative aspect, namely the changes in the intracellular concentrations of MAPs due to the microinjection, we have made the following rough estimations: in the neuronal cells, namely NBr10-A, the concentration of MAP₂ was found to be ~1% of the total cytosolic proteins by densitometric analysis of proteins fractionated by PAGE (data not shown). If we assume that total cellular protein concentration is ~50–100 mg/ml and a total cell volume of ~4 × 10⁻¹² liter, then the number of MAP₂ molecules (270,000 mol wt) is ~5 × 10⁶/cell. In non-neuronal cells, on the other hand, controversy still exists with respect to the presence of authentic MAP₂ or functionally related proteins (45–47; for review, see reference 48). In the extreme case, if we consider the possibility that cultured chicken gizzard fibroblasts or PtK₂ cells do not contain MAP₂ we must reach the conclusion that nevertheless their microtubules display the capacity to bind brain MAP₂. This would suggest that the binding sites for MAP₂ are conserved regardless of the presence or absence of this protein in the cells. Assuming that MAP₂ does exist in a wide variety of non-neuronal cells, though in low concentrations (<0.04% of the total cellular proteins (47)), then the maximal number of MAP₂ molecules per cell would be of the order of 10⁵. The estimated volume microinjected into individual cells is ~10⁻¹³ (37) liters and the concentration of MAP₂ is 1.5 mg/

ml (5.6 × 10⁻⁶ M). Thus the number of molecules introduced into individual cells would be about 3.5 × 10⁵ per cell. This implies that, while in the neuroblastoma-liver hybrid cells we increase the MAP₂ concentration by 15%, the relative increase in non-neuronal cells would be three- to fourfold compared to the endogenous pool of MAP₂. Nevertheless it should be emphasized that in all these cells the amount of microinjected MAPs was lower than that required to saturate all cellular tubules assuming that saturation is achieved at 1:6 molar ratio of MAP₂ to tubulin (49). However, in view of the possible effect of MAP₂ concentration on microtubule dynamics we have chosen here to study the mobility of MAP₂ in NBr10-A cells where authentic MAP₂ is present and its concentration is only slightly changed by the injection, as pointed above.

The results described here indicate that in living cells (PtK₂, NBr10-A, and chicken gizzard cells) MAP₂ associates predominantly with microtubules. This conclusion is not trivial in view of the putative role of MAP₂ as a linker of microtubules to other cytoplasmic elements. Thus, if indeed MAP₂ is involved in such interactions, it probably associates with much higher affinity with microtubules than with other structures. Of special relevance is the observation that AF-MAP₂ is not associated with vimentin or prekeratin in PtK₂ cells. This cannot exclude the possibility that other intermediate filaments (neurofilaments, for example) do bind MAP₂, or that the interaction with I-AF selectively reduced MAP₂-binding capacity to other cell organelles.

The results described here also suggest that the binding of the AF-MAPs to native microtubules *in vivo* occurs in a wide variety of cells. There are two additional structures with which the injected AF-MAP₂ became associated in our experiments: microtubule-organizing centers and vinblastine-induced paracrystals. Nevertheless generally the entire microtubular system incorporated AF-MAP₂ to a similar extent suggesting that microtubules may bind the associated proteins along their entire length.

The dynamic parameters of MAP₂-microtubules interaction were investigated by the FPR method. The results indicated that after photobleaching of microtubule bundles in NBr10-A cells or defined individual microtubules in other cell types a recovery of fluorescence occurred. Since the fluorophore is irreversibly bleached, the recovery of fluorescence following photobleaching indicates that new cytoplasmic MAPs were incorporated into the bleached area. This process and its particular rate was not affected by the type of cell used, the intrinsic content of MAP₂, the time interval between microinjection and photobleaching and the size of the photobleached region. The photobleaching data also clearly showed that MAP₂ can be incorporated into preexisting microtubules along their length in a polymerization-independent fashion. It should be emphasized that the measurements were performed with minimal intensities of the bleaching beam to prevent or minimize the damage to the microtubules at the site of bleaching. Indeed immunolabeling of cells with tubulin antibodies immediately after bleaching did not reveal any sign for discontinuity of the microtubules in these areas (data not shown).

Do Microtubules Undergo Treadmilling In Vivo?

Several studies (16–19, 21, 22) over the last few years indicated that under defined *in vitro* conditions, there is a flux of tubulin subunits along the microtubule backbone from

the plus end towards the minus end (for extensive discussion, see references 19, 22). The rates of treadmilling reported for different experimental systems showed a wide variability, ranging from 0.7 (21) to 50 $\mu\text{m}/\text{h}$ (18). Factors that had significant effects on the apparent rate of treadmilling were the source of tubulin, buffer used, concentration of monomers, temperature and the presence of MAPs and their apparent phosphorylation (19). One of the attractive features of the treadmilling models is that they provide tentative explanation for a variety of dynamic cellular processes in which microtubules are believed to participate. These include chromosome movements, possible mobilization of pigment granules, and mitochondria (19).

Any attempt to associate treadmilling mechanisms with mobilization of cytoplasmic structures must take into account the presence of MAPs. These proteins (especially MAP₂) are associated peripherally with the tubulin backbone and most likely mediate at least some of the interactions in which microtubules are involved (26, 27). One could predict, therefore, that if treadmilling of tubulin serves as a driving force for organelle translocation, it would also mobilize MAP₂ along the microtubules. This theoretical possibility of treadmilling-dependent co-translocation of tubulin and MAP₂ is schematically shown in Fig. 8A. Our results however, do not support such a model. We have shown here that the bleached spot on AF-MAPs bound to microtubules does not appear to move and the fluorescence on the bleached area recovers by exchange of MAPs with the surrounding soluble pool. It should be clearly emphasized that treadmilling $<3\text{--}5 \mu\text{m}/\text{h}$, even if it carries MAP₂ along, could not be detected in our system. Moreover, the mechanism shown in Fig. 8A is incompatible with the fact that the slow fluorescence recovery of AF-MAPs occurs along the entire length of the microtubules and not at their ends.

Fig. 8B illustrates a mechanism in which treadmilling may occur in the tubulin backbone while MAP₂ is not carried along due to either interactions with other stationary cytoplasmic structures or to sliding movement of MAP₂ relative to microtubules. In the absence of direct evidence on the dynamics of pure tubulin, we cannot rule out this possibility (our attempts to purify labeled tubulin yielded a probe with reduced capacity to polymerize and to be incorporated into fibers). However, in view of the long residence time of AF-MAP₂ towards microtubules in living cells we consider this alternative unlikely.

The injection of AF-MAPs did not change the morphological appearance of cells nor did it affect cell division or the duration of the mitotic cycle (B. Vandenbunder and G. G. Borisy, unpublished observations). These observations do not support the possibility that injection of exogenous AF-MAP₂ causes immobilization of the microtubules.

Fig. 8, C and D, illustrate mechanisms in which there is no detectable treadmilling. Fig. 8C shows an exchange of MAP₂ and tubulin subunits between the assembled microtubules and the soluble cytoplasmic pools, whereas Fig. 8D shows the exchange for MAP₂ only. We think the possibility illustrated by Fig. 8C is unlikely because it implies tubulin exchange along the length of the microtubule, whereas all the available data indicate that exchange is restricted to the ends of the microtubule (40, 50–52). This leaves us with the scheme of Fig. 8D as an adequate explanation of the FPR results, namely exchange of the MAP molecules without the involvement of the treadmilling process.

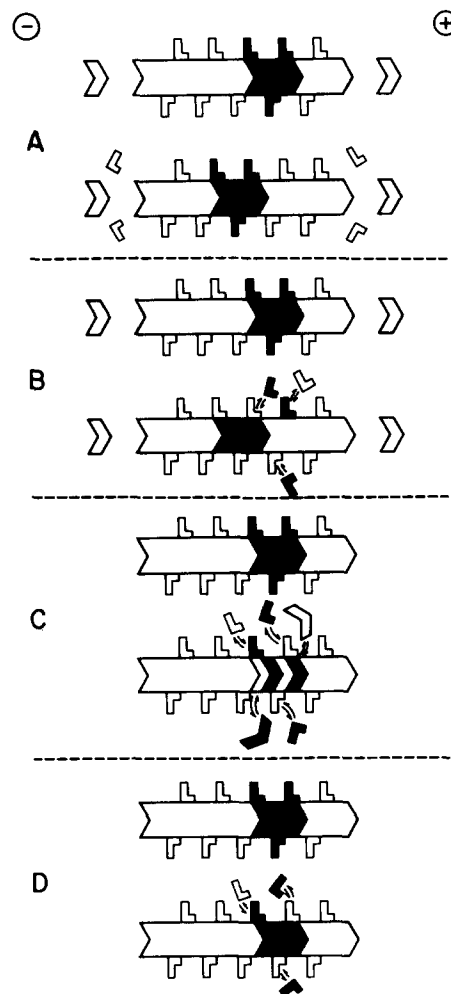


FIGURE 8 Models representing the interrelationships between the soluble pool of tubulin and MAP₂ and the microtubule. In these models, the chevrons illustrate tubulin dimers while the L-shaped rods correspond to MAP₂ molecules. For each of the models the same microtubular components (marked with black) are shown at two time points. The possibilities put forward are the following: (A) Treadmilling may occur in the tubulin backbone while MAP₂ remains immobile but exchanges, possibly due to interactions with other cytoplasmic structures or to sliding activity. (C) Treadmilling does not take place. Both MAP₂ and tubulin exchange between the assembled microtubules and the soluble cytoplasmic pool. (D) Treadmilling does not take place. Only MAP₂ exchanges with the soluble cytoplasmic pool.

Further experiments will be necessary to determine if treadmilling occurs at rates below the threshold detectable in this study. We expect that the experimental strategy outlined here will be employed in the future for examination of the dynamic properties of tubulin itself. Such experiments, if performed with biologically active tubulin, may indicate whether detectable treadmilling occurs along the tubulin backbone in living cells.

T. E. Kreis was a recipient of a long-term European Molecular Biochemical Organization Fellowship. This work was supported in part by the U.S. Binational Science Foundation, (U. Z. Littauer and J. Schlessinger), the Muscular Dystrophy Association grant (to U. Z. Littauer and B. Geiger), from the National Institutes of Health (CA-25820 to J. Schlessinger and GM 25062 to G. G. Borisy), and from Stiftung Volkswagenwerk (J. Schlessinger). B. Geiger was an incumbent of the Charles Revson Chair in Biology.

REFERENCES

1. Roberts, K., and J. S. Hyams, editors. 1979. Microtubules. Academic Press, Inc., NY.
2. Cleveland, D. W., S. Y. Hwo, and M. H. Kirschner. 1977. Purification of Tau, a microtubules associated protein which induces assembly of microtubules from purified tubulin. *J. Mol. Biol.* 116:227-248.
3. Murphy, D. B., and G. G. Borisy. 1975. Association of high molecular weight proteins with microtubules and their role in microtubule assembly *in vivo*. *Proc. Natl. Acad. Sci. USA* 72:2696-2700.
4. Sloboda, R. D., W. L. Dentler, and J. L. Rosenbaum. 1976. Microtubule associated proteins and the stimulation of tubulin assembly *in vitro*. *Biochemistry* 15:4497-4505.
5. Weingarten, M. D., A. H. Lockwood, S. Hwo, and M. W. Kirschner. 1975. A protein factor essential for microtubule assembly. *Proc. Natl. Acad. Sci. USA* 72:1858-1862.
6. Bulinski, J. C., and G. G. Borisy. 1980. Immunofluorescence localization of HeLa cell microtubule-associated proteins on microtubules *in vitro* and *in vivo*. *J. Cell Biol.* 87:792-801.
7. Connolly, J. A., V. I. Kalnins, D. W. Cleveland, and M. W. Kirschner. 1978. Intracellular localization of the high molecular weight microtubule accessory protein by indirect immunofluorescence. *J. Cell Biol.* 76:R781-R786.
8. Sherline, P. 1978. Localization of the major high molecular weight protein on microtubules *in vitro* and in cultured cells. *Exp. Cell Res.* 115:460-464.
9. Sherline, P., and K. Schiavone. 1977. Immunofluorescence localization of high molecular weight proteins along intracellular microtubules. *Science (Wash. DC)* 198:1038-1040.
10. Fellous, A., J. Francon, A. Lennon, and J. Nunez. 1977. Microtubule assembly *in vitro*. Purification of assembly-promoting factors. *Eur. J. Biochem.* 78:167-174.
11. Murphy, D. B., K. A. Johnson, and G. G. Borisy. 1977. Role of tubulin-associated protein in microtubules nucleation and elongation. *J. Mol. Biol.* 117:33-52.
12. Inoue, J., and H. Sato. 1967. Cell motility by labile association of molecules. The nature of mitotic spindle fibers and their role in chromosome movement. *J. Gen. Physiol.* 50:259-292.
13. McIntosh, J. R., P. K. Hepler, and D. G. Van Wic. 1969. Model for mitosis. *Nature (Wash. DC)* 224:699-663.
14. F. D. Warner. 1976. Cross-bridge mechanisms in ciliary motility: the sliding-bending conversion. *Cold Spring Harbor Conf. Cell Proliferation* 3(Book A): 891-914.
15. Murphy, D. B., and L. G. Tilney. 1974. The role of microtubules in the movement of pigment granules in teleost melanophores. *J. Cell Biol.* 61:757-779.
16. Allen, C., and G. G. Borisy. 1974. Structural polarity and directional growth of microtubules of *Chlamydomonas* flagella. *J. Mol. Biol.* 90:381-402.
17. Bergen, L. G., and G. G. Borisy. 1980. Head-to-tail polymerization of microtubules *in vitro*: electron microscope analysis of seeded assembly. *J. Cell Biol.* 84:141-150.
18. Cote, R. H., and G. G. Borisy. 1981. Head-to-tail polymerization of microtubules *in vitro*. *J. Mol. Biol.* 150:577-602.
19. Margolis, R. L., and L. Wilson. 1981. Microtubules treadmills—possible molecular machinery. *Nature (Lond.)* 293:705-711.
20. Wegner, A. G. 1976. Head-to-tail polymerization of actin. *J. Mol. Biol.* 108:139-150.
21. Margolis, R. L., and L. Wilson. 1978. Opposite end assembly and disassembly of microtubules at steady state *in vitro*. *Cell* 13:1-8.
22. Kirschner, M. 1980. Implications of treadmilling for the stability and polarity of actin and tubulin polymerization *in vivo*. *J. Cell Biol.* 86:330-334.
23. Ball, E. H., and S. J. Singer. 1982. Mitochondria are associated with microtubules and not with intermediate filaments in cultured fibroblasts. *Proc. Natl. Acad. Sci. USA* 79:123-126.
24. Geiger, B., and S. J. Singer. 1980. Association of microtubules and intermediate filaments in chicken gizzard cells as detected by double immunofluorescence. *Proc. Natl. Acad. Sci. USA* 77:4769-4773.
25. Schliwa, M. 1979. Stereo high voltage electron microscopy of melanophores. *Exp. Cell Res.* 118:323-340.
26. Griffith, L. M., and T. D. Pollard. 1978. Evidence for actin filament-microtubule interaction mediated by microtubule-associated proteins. *J. Cell Biol.* 78:958-965.
27. Schliwa, M., and J. van Blerkom. 1981. Structural interaction of cytoskeletal components. *J. Cell Biol.* 90:222-235.
28. Taylor, D. L., and Y. L. Wang. 1978. Molecular cytochemistry: incorporation of fluorescently labeled actin into living cells. *Proc. Natl. Acad. Sci. USA* 75:857-861.
29. Kreis, T. E., K. H. Winterhalter, and W. Birchmeier. 1979. *In vivo* distribution and turnover of fluorescently labeled actin microinjected into human fibroblasts. *Proc. Natl. Acad. Sci. USA* 76:3814-3818.
30. Keith, C. H., J. R. Feramisco, and M. Shelanski. 1980. Direct visualization of fluorescein-labeled microtubules *in vitro* and in microinjected cells. *J. Cell Biol.* 88:234-240.
31. Feramisco, J. R. 1979. Microinjection of fluorescently labeled α -actinin into living fibroblasts. *Proc. Natl. Acad. Sci. USA* 76:3967-3971.
32. Burridge, K., and J. R. Feramisco. 1980. Microinjection and localization of a 130K protein in living fibroblasts: a relationship to actin and to fibronectin. *Cell* 19:587-595.
33. Kreis, T. E., B. Geiger, and J. Schlessinger. 1982. Mobility of microinjected rhodamine actin within living chicken gizzard cells determined by fluorescence photobleaching recovery. *Cell* 29:835-845.
34. Geiger, B., L. Avnur, T. E. Kreis, and J. Schlessinger. 1984. The dynamics of cytoskeletal organization in areas of cell contact. *Cell Muscle Motil.* In press.
35. Kreis, T. E., T. Scherson, U. Z. Littauer, J. Schlessinger, and B. Geiger. 1982. Dynamics of microtubules in living cultured cells. *J. Cell Biol.* 95(2, Pt. 2):348a. (Abstr.)
36. Nirenberg, M., S. Wilson, H. Higashida, A. Rotter, K. Krueger, N. Busis, R. Ray, J. G. Kenimer, and M. Adler. 1983. Modulation of synapse formation by cyclic adenosine monophosphate. *Science (Wash. DC)* 222:794-799.
37. Kreis, T. E., and W. Birchmeier. 1982. Microinjection of fluorescently labeled proteins into living cells, with emphasis on cytoskeletal proteins. *Int. Rev. Cytol.* 75:209-227.
38. Shelanski, M. L., F. Gaskin, and C. R. Cantor. 1973. Microtubule assembly in the absence of added nucleotides. *Proc. Natl. Acad. Sci. USA* 70:765-768.
39. Axelrod, D., D. E. Koppel, J. Schlessinger, E. L. Elson, and W. W. Webb. 1976. Mobility measurements by analysis of fluorescence photobleaching recovery. *Biophys. J.* 16:1055-1069.
40. Nagle, D. W., and J. Bryan. 1976. Factors affecting nucleation and elongation of microtubules *in vitro*. *Cold Spring Harbor Conf. Cell Proliferation* 3(Book A):1213-1232.
41. Laemmli, U. K. 1970. Cleavage of structural proteins during the assembly of the head of bacteriophage T₄. *Nature (Lond.)* 227:680-685.
42. Schliwa, M., U. Euteneuer, J. C. Bulinski, and J. G. Izant. 1981. Calcium lability of cytoplasmic microtubules and its modulation by microtubule associated proteins. *Proc. Natl. Acad. Sci. USA* 78:1037-1041.
43. Scherson, T., B. Geiger, Z. Eshhar, and U. Z. Littauer. 1982. Mapping of distinct structural domains on microtubule-associated protein 2 by monoclonal antibodies. *Eur. J. Biochem.* 129:295-302.
44. Connolly, J. A., and V. I. Kalnins. 1980. TAU and HMW microtubule-associated proteins have different microtubule binding sites *in vivo*. *Eur. J. Cell Biol.* 21:296-300.
45. Bulinski, J. C., and G. G. Borisy. 1980. Wide spread distribution of a 210,000 molecular weight microtubule associated protein in cells and tissues of primates. *J. Cell Biol.* 87:802-808.
46. Bulinski, J. C., and G. G. Borisy. 1980. Microtubule associated proteins from cultured HeLa cells. Analysis of molecular properties and effects of microtubule polymerization. *J. Biol. Chem.* 255:11570-11576.
47. Weatherbee, J. A., P. Sherline, R. N. Mascardo, J. G. Izant, R. B. Lufting, and R. R. Weising. 1982. Microtubule-associated proteins of HeLa cells: heat stability of the 200,000 mol wt HeLa MAPs and detection of the presence of MAP₂ in HeLa cell extracts and cycled microtubules. *J. Cell Biol.* 92:155-163.
48. Littauer, U. Z., and I. Ginzburg. 1984. Expression of microtubule proteins in brain. *In Gene Expression in Brain*. C. Zomzely-Neurath and W. A. Walker, editors. J. Wiley and Sons, N.Y. In press.
49. Vallee, R. B., and G. G. Borisy. 1978. The non-tubulin component of microtubule protein oligomers. *J. Biol. Chem.* 253:2834-2845.
50. Johnson, K. A., and G. G. Borisy. 1977. Kinetic analysis of microtubule assembly *in vitro*. *J. Mol. Biol.* 117:1-31.
51. Margolis, R. L., and L. Wilson. 1978. Opposite end assembly and disassembly of microtubules at steady-state *in vitro*. *Cell* 13:1-8.
52. Bergen, L. G., and G. G. Borisy. 1980. Head-to-tail polymerization of microtubules *in vitro*. *J. Cell Biol.* 84:141-150.